

Distribution Agreement

In presenting this thesis as a partial fulfillment of the requirements for a degree from Emory University, I hereby grant to Emory University and its agents the non-exclusive license to archive, make accessible, and display my thesis in whole or in part in all forms of media, now or hereafter now, including display on the World Wide Web. I understand that I may select some access restrictions as part of the online submission of this thesis. I retain all ownership rights to the copyright of the thesis. I also retain the right to use in future works (such as articles or books) all or part of this thesis.

Cory Sylber

April 11, 2019

Scavenger Receptor Expression is Differentially Affected by DNAzyme-Gold Nanoparticle
Conjugates in a Lung Model

By

Cory Sylber

Dr. Cherry Wongtrakool, M.D.
Adviser

Department of Chemistry

Dr. Cherry Wongtrakool, M.D.
Adviser

Dr. Khalid Salaita, Ph.D.
Committee Member

Dr. José Soria, Ph.D.
Committee Member

2019

Scavenger Receptor Expression is Differentially Affected by DNAzyme-Gold Nanoparticle
Conjugates in a Lung Model

By

Cory Sylber

Dr. Cherry Wongtrakool, M.D.

Adviser

An abstract of
a thesis submitted to the Faculty of Emory College of Arts and Sciences
of Emory University in partial fulfillment
of the requirements of the degree of
Bachelor of Sciences with Honors

Department of Chemistry

2019

Abstract

Scavenger Receptor Expression is Differentially Affected by DNAzyme-Gold Nanoparticle Conjugates in a Lung Model

By Cory Sylber

Scavenger receptor (SR) surface proteins are highly conserved motifs and are implicated in the uptake of conjugated DNAzyme-nanoparticles (DzNP), a promising novel nanotherapy for lung diseases. The role of SRs in DzNP uptake in the lung is poorly understood, so we examined whether DzNP exposure and uptake regulates gene expression in murine alveolar macrophages and primary human airway epithelial cells. Gene expression is modulated by 2251DzNP in both MH-S cells and NhTE cells, suggesting that 2251DzNP may facilitate its own uptake, but the extent to which each SR is affected depends heavily on its class and involvement in inflammation signaling pathways. This represents novel findings in lung tissue that support previous work done on nanotherapy uptake and influences the development of novel therapies for lung diseases.

Scavenger Receptor Expression is Differentially Affected by DNAzyme-Gold Nanoparticle
Conjugates in a Lung Model

By

Cory Sylber

Dr. Cherry Wongtrakool, M.D.

Adviser

A thesis submitted to the Faculty of Emory College of Arts and Sciences
of Emory University in partial fulfillment
of the requirements of the degree of
Bachelor of Sciences with Honors

Department of Chemistry

2019

Acknowledgements

Foremost, I would like to express my gratitude to my adviser, Dr. Cherry Wongtrakool, for providing me with the opportunity to conduct a thesis project in her laboratory, guiding me in my scientific exploration as an undergraduate, and serving as a mentor who I trust and admire. I would like to also thank my committee members, Dr. José Soria and Dr. Khalid Salaita, both of whom provided valuable feedback to me throughout editing and revising my thesis. I would like to extend my appreciation to Dr. Khalid Salaita, and the Salaita Lab as a whole, for working in conjunction with me to keep the project heading forward; their collaboration was instrumental to conducting my research.

Additionally, I would like to thank Emory University and the Department of Chemistry for providing undergraduate students, like myself, the avenues to explore science through research.

Finally, I would like to thank Emory University School of Medicine and the Department of Veterans Affairs for providing the resources and funding necessary to conduct my research. I am immensely grateful for the assistance provided by all agencies which helped fund my research: Emory SURE Program, Emory School of Medicine Seed Grant, National Institutes of Health, and the Department of Veterans Affairs. I would like to give special recognition to the CF@LANTA Experimental Models Support Core for procuring the normal human primary epithelial cells.

Table of Contents

List of Figures.....	ii
List of Abbreviations.....	ii
I. Introduction.....	1
II. Materials and Methods.....	8
1.1. <i>Materials</i>	8
1.2. <i>Gold nanoparticle synthesis</i>	8
1.3. <i>DNAzyme-gold nanoparticles functionalization</i>	8
1.4. <i>Cell culture</i>	9
1.5. <i>Particle uptake by macrophages</i>	10
1.6. <i>In vitro gene expression</i>	11
1.7. <i>Statistics</i>	11
III. Results	12
1.1. <i>MARCO and MSR1 Gene Expression with Dose Response to DSS and DzNP in MH-S Cells</i>	12
1.2. <i>MARCO and MSR1 Gene Expression for Concomitant 2251DzNP and low MW DSS in MH-S Cells</i>	14
1.3. <i>Low Dose 2251DzNP Expression Levels in MH-S Cells</i> :.....	16
1.4. <i>MSR1 Expression in NhTE Cells with Concomitant Treatment</i>	17
1.5. <i>CD36 and COLEC12 Expression in NhTE Cells with Concomitant Treatment</i>	18
1.6. <i>MH-S Particle Uptake</i>	19
IV. Discussion	20
V. References	24

List of Figures

Figure 1.....	12
Figure 2.....	13
Figure 3.....	14
Figure 4.....	15
Figure 5.....	16
Figure 6.....	17
Figure 7.....	18
Figure 8.....	19

List of Abbreviations

Collagen Type I Receptor, Thrombospondin Receptor	CD36
Collectin Subfamily Member 12	COLEC12
dextran sodium sulfate	DSS
DNAzyme-nanoparticle	DzNP
gold nanoparticle	AuNP
Macrophage Receptor with Collagenous Structure	MARCO
Macrophage Scavenger Receptor 1	MSR1
microRNA	miRNA
molecular weight	MW
nanoparticle	NP
nanomaterial	NM
polymerase chain reaction	PCR
RNA interference	RNAi
small interfering RNA	siRNA

I. Introduction

The field of nanotechnology encompasses the manipulation of nanomaterials (NM) at the near-atomic scale to create structures with useful properties[1]. NM properties are distinct from the predicted bulk properties, most notably the mechanical, optical, and electrical behaviors[2, 3]; understanding the properties of nanomaterials has yielded influential inventions such as semiconductor transistors in electronics, dialysis films for kidney disease treatment, and fullerenes in nuclear imaging. Nanoparticles (NP) are a subset of NMs that have nanometer dimensions in all directions, ranging from 1-100nm, and exist in a myriad of shapes, such as spheres, rods, and hollow wires[4]. The advent of field emission microscopy (FEM) made it possible to image the crystallographic arrangement of nanomaterials at a near-atomic scale[5]. Through further development of imaging techniques and analysis methods, it became easier to predict and manipulate the unique properties of NPs[6]. The unique properties of NPs provide noteworthy advantages compared to traditional materials or mixtures and can be employed to tackle current challenges in medicine.

Many NPs were initially developed by industry to serve aims such as purification of crude oil, physical UV protectants, and antimicrobial/burn treatment therapies[7-9]. The success of these NPs substantially benefited the field by showing the breadth of application that NPs have towards enhancing conventional technologies. NPs represent an important nanotechnology due to their distinct surface-to-volume ratio, making them suitable for dispersing chemically reactive substances in a remarkably efficient manner[10]. NPs are identified based on their dimensions, morphology, composition, uniformity, and

agglomeration[11]. An NPs' dimensions enhance their ability to move in the environment compared to a bulk solution and its elemental/molecular composition largely contribute to the nano-properties that can be exploited, such as magnetism, plasmonic enhancement effects, and catalytically active surfaces. The morphology of NPs can drastically change the behavior in a given environment, namely how they will be dispersed[12]. Control of NP's distribution and uniformity in a system allows focused, macroscopic effects to be deliberately chosen, such as dispersal in biological systems.

NPs are not relegated to human-made materials. Recently, biologically significant macromolecules have been considered nanomaterials due to their size and the ability to control the properties they exhibit at the nanoscale[13]. DNA has nanomaterial properties with its relative size and robust applications in biological systems. DNA's diameter is 2nm and its pitch is 3.4nm; varying strand lengths from a few dozen base pairs to hundreds of millions allow DNA to create complex conformations – such as supercoiling and aptamer binding – and substantially increases the diversity of DNA as a nanomaterial [14]. Because DNA production is no longer dependent on cell-based machinery and can be synthesized in an exponential span of sequences, use of DNA as a NM has virtually infinite possibilities for biological applications.

Because DNA codes the genes for proteins essential for cellular operations, DNA is a compelling material for NM development. To create these proteins, messenger RNA (mRNA) encoding the amino acid sequence is transcribed from the DNA in the nucleus before it reaches the protein biosynthesis machinery. To inhibit protein synthesis, gene silencing must occur either at the DNA level in the nucleus, or at the transcriptional level by targeting mRNA [15]. Several oligonucleotide structures are capable of targeting mRNA. A catalytic

RNA molecule (ribozyme) was discovered and subsequently yielded a plethora of non-coding miRNA capable of interfering with mRNA translation [16]. These non-coding strands are typically folded back on themselves into short hairpin-loops that carry out gene silencing aided by additional cell machinery. Akin to miRNA is siRNA, which is a dsRNA complex that carries out gene silencing without the need for additional cell machinery that miRNA needs[17]. Additional methods of RNA interference (RNAi) have been developed to silence genes in a similar fashion to si/miRNA[18]. However, because the cellular environment is primed to degrade and recycle RNA constructs, the direct application of RNA-based gene silencing as a human therapeutic is currently limited.

Efforts to expand the repository of RNAi methods led to the discovery of DNA sequences that catalyzed reactions, akin to ribozymes[19, 20]. These deoxyribozymes (DNAzymes), while not found in nature, improve the catalytic diversity of nucleic acids due to increased stability of DNAzymes, owed in part to the 3'-deoxyribose backbone of DNA[21]. DNAzymes that require an Mg^{2+} cofactor are among the most widely studied, specifically those with a 15-base pair catalytic core flanked on either side by binding domains (10-23 DNAzymes) that cleave complementary RNA strands between a purine-pyrimidine pair[22-24]. 10-23 DNAzymes all contain a conserved catalytic domain with variable binding domains; the target site specificity has unprecedented tunability and represents a powerful tool for RNAi-like inactivation as the binding domain boasts substrate discrimination on the same, if not greater, order as ribozymes and synthetic RNAi[25]. The advantages DNAzymes possess versus traditional RNAi methods are a two-fold product of DNA's chemical structure: first, the catalytic core and active site can physically get closer to the substrate due to the 3'-deoxy substituents; second, only complementary DNAzyme-substrate display catalytic

activity – any mismatches in the purine-pyrimidine cleavage site have virtually no activity[26, 27]. As a result, the use of DNA over RNA improves key modalities of RNA silencing pathways such as chemical stability, endonuclease resistance, and preferentially adopting duplexes.

A high-throughput directed selection method is carried out *in vitro* to select specific DNA sequences possessing catalytic activity for a desired substrate, such as IGF-1, GATA-3, and TNF- α [28-30]. DNAzymes are selected in conditions similar to biologically relevant conditions. DNAzymes can be used to downregulate the genes associated with disease pathways, such as cancer, inflammation diseases, and bacterial infection[31-33]. With its RNAi-like activity, DNAzymes can also act as biological sensors to make new tools that are both therapeutic and diagnostic (theranostic)[34]. However, free DNAzymes are limited by their ability to readily enter cells, which is a significant barrier in multicellular organisms. Facilitating cellular uptake of DNAzymes is essential to remedy this obstacle. One remedy is to modify the DNAzyme molecule to increase uptake. Conjugating DNAzymes to a NP to yield a new functional unit is one modification that improves cellular uptake compared to non-conjugated DNAzymes[35].

NPs conjugated with catalytically active DNAzymes are DNAzyme-nanoparticles (DzNP) and constitute a large portion of nanozymes in research and development[28, 36, 37]. Gold is routinely chosen as the NP to conjugate DNAzymes because it has been studied extensively and it makes ideal scaffolds to build functionality due to their high stability, well studied plasmonic effects, good catalytic activity, and low cytotoxicity compared to other metals[38]. Gold nanoparticles (AuNP) are synthesized with a diameter of 10-15nm and functionalized with the DNAzymes on the outside. The DNAzyme improves the solubility of the AuNP by

providing it with surface charge and stabilizes the colloid solution while preserving its shelf-life. Gold's affinity for sulfur is exploited by chemically modifying the DNAzyme with a short polyethylene glycol (PEG) chain with a terminal thiol group to promote conjugation.

Many RNA cleaving DNAzymes have been conjugated to AuNPs and tested for their efficacy to downregulate expression levels in vivo, such as NS3 knockdown in acute hepatitis C infections[39, 40]. In comparison to the free DNAzyme counterpart, many DzNPs show increased catalytic activity, increased bioavailability through elevated cellular uptake, and diminished cytotoxicity[41]. DzNPs offer novel treatment approaches for human pathologies like cancer, viral infections, and autoimmune diseases, and they achieve this by improved delivery of DNAzymes and target specificity[30, 42]. When compared to traditional RNA inhibition, the inflammatory response of DzNPs is significantly reduced and potentially confers therapeutic advantage, but further investigation into potential toxicity is still needed. Since cellular uptake efficiency directly influences toxicity, understanding the mechanisms of DzNP uptake into the cell is crucial to advancing the therapeutic potential of DzNPs.

Scavenger receptors (SR) are part of a large, structurally diverse protein family primarily expressed by myeloid cells and serve to help remove foreign material that are identified as non-self[43-45]. SRs also recognize a diverse set of ligands including microbial pathogens and modified small biomolecules such as lipoproteins. SRs are components of several import mechanisms, including endocytosis, cell-cell adhesion, and signal transduction, to eliminate foreign substances[44, 46]. The most studied SRs are Scavenger Receptor Class-A (SR-A): membrane-bound proteins with a short transmembrane domain and large extracellular domains, which permit recognition of a wide range of ligands. Unique to SR-A are SR cysteine-rich (SR-CR) domains on the terminus, preceded by a collagen-like domain,

followed by the α -helical coiled-coil domain[44]. SR-As are most abundant on macrophages, but endothelial cells that experience high levels of oxidative stress also express a significant amount of SR-As. The binding domains of all SR-As have a high affinity for multivalent, anionic polymers; for example, lipopolysaccharides (LPS) on bacteria's surfaces stimulates SR-A upregulation in macrophages[47]. SR-As in leukocytes have been implicated in the binding and uptake of β -amyloid, molecular surface patterns on Gram-positive/negative bacteria, and hepatitis C viral capsid[47-49].

SR-As are integral to cellular adherence to nanosurfaces and SR-As are implicated in the uptake of NPs of spherical morphology and diameter 10-15nm[50, 51]. The results of a double knockout murine lineage lacking both SR-A1 (MSR1) and SR-A6 (MARCO) in alveolar macrophages (AM) had a reduced ability to bind and ingest NPs[33]. MSR1 and MARCO both aid in initiating endocytosis of bacteria in the lungs. SR-As recognize nucleic acids as another polyanionic substrate and the coiled-coil domain of SR-A1/A6 directly binds dsDNA and ssDNA, thus implicating the role of SR-A1/A6 for internalizing exogenous DNA[52]. Based on the currently available data, SR-A1 and SR-A6 are likely involved in the internalization of DzNPs.

The functions of SRs, particularly SR-As, has been extensively studied since SR-As are conserved across nearly all mammalian cells. However, very little is known about SR function in lung cells other than alveolar macrophages. Macrophages and airway epithelial cells are the first cells that will encounter DzNPs in the lung when delivered via inhalation. Previous work demonstrates that naked DNazymes can be safely administered to the lung via inhalation as a potential therapy for asthma[29, 53, 54]. Therefore, DzNP-SR interactions are

critical to examine to understand how inhaled delivery of DzNPs regulates gene expression in the lung.

Previous work from this lab demonstrated that DzNPs confer significant advantage over naked DzNPs due to improved cellular uptake in macrophages[25]. A novel DzNP catalyzing degradation of GATA-3 mRNA (subsequently referred to as 2251DzNP) holds promise in the treatment of asthma. Because inhalation is a highly preferred method of delivery over systemic delivery, the experiments presented herein use a murine alveolar macrophage cell line (MH-S) and primary human airway epithelial cells to study DzNP-SR interactions in the lung. In particular, we investigate the effects of 2251DzNP on scavenger receptor expression. In anticipation of using dextran sodium sulfate (DSS) as a SR inhibitor, we also investigated the effects of DSS on scavenger receptor expression using both high molecular weight DSS (to mimic the size of a NP) and low molecular weight DSS (to mimic the polyanionic charge of DNA)[55-59].

II. Materials and Methods

- 1.1. *Materials*: Nanopure water [18.3M Ω] was used for AuNP synthesis, which were then stabilized with chemicals from Sigma-Aldrich. The RNA isolation kits (*mirVana*[™] miRNA Isolation Kit) from Invitrogen (Thermo Fisher Scientific, Waltham, MA) and TRIzol[®] Reagent from Ambion[®] (Life Technologies[™], Carlsbad, CA; now Invitrogen of Thermo Fisher Scientific, Waltham, MA) used for RNA isolation were purchase from the respective companies. Complementary DNA (cDNA) synthesis kits (*iScript*[™] cDNA Synthesis Kit) were obtained from Bio-Rad Laboratories for generating cDNA from total RNA isolate. The oligonucleotides used were purchased from Integrated DNA Technologies, Inc (IDT) in μ mole amounts using standard phosphoramidite methods.
- 1.2. *Gold nanoparticle synthesis*: The AuNPs were synthesized according to previously published procedure[60]. A 500 mL, 1 mM hydrogen tetrachloroaurate(III) trihydrate solution was brought to a boil, refluxing at atmospheric pressure; upon boiling, 50mL of a sodium citrate tribasic dihydrate solution at 38.8mM was added, after which the solution was allowed to continue to reflux for 15 minutes. Isolation of the desired AuNP size (13 nm) was achieved by vacuum filtration through a 0.45 mm acetate filter, whereby the monodispersed AuNP's size was determined by transmission electron microscopy (TEM) and the concentration obtained by UV-vis absorbance spectroscopy (NanoDrop[™] Spectrophotometer, Thermo Fisher Scientific).
- 1.3. *DNAzyme-gold nanoparticles functionalization*: Modified oligonucleotides with disulfide termini from IDT were incubated for 3 hours with disulfide cleavage buffer

(0.1M dithiothreitol (DTT); 170 mM phosphate buffer; pH 8.0) to render a free thiol at the terminus. Using NAP-25 columns (GE Healthcare, Piscataway, NJ) and NanoPure water as the eluent, the reduced oligos were purified, whereby the concentration was determined. Once purified, 4 nmol oligo were added per 1 mL of AuNP solution, yielding a solution with AuNP and oligo concentration of ~10-15 nM and ~2.5-3.5 nM, respectively. The solution was left on an orbital shaker overnight (~8 h), after which 10x stock phosphate buffer solution (PBS), 10x stock sodium dodecyl sulfate (SDS) buffer solution, and 8 successive stock sodium chloride (NaCl) partitions were sequentially added to bring the final concentrations of the AuNPs to 9 mM PBS, 0.1% (g/mL) SDS, and 0.7 M NaCl. The fully salted DNA-AuNP solution was placed on an orbital shaker in the dark overnight to yield the desired DNAzyme-AuNP conjugate (DzNP). The DzNP stock solution was stored in these conditions at 4°C (keeping for ~1 month, until needed). Particles were washed by 3 successive additions of NanoPure water and centrifugation at 13,500 RPM after initially spun down from the stock solution. Particles were reconstituted in 1x PBS for application and kept for ~1 week.

1.4. *Cell culture*: The murine alveolar macrophage cell line used – MH-S (ATCC® CRL 2019™) cells – were from a seed stock initially obtained from American Type Culture Collection (ATCC #: CRL 2019). Working stocks were generated by thawing cells that were previously cryopreserved according to standard protocols. Cells were maintained in a 37°C, 5% CO₂, humidified incubator and grown in Roswell Park Memorial Institute (RPMI) media (Gibco™ RPMI Medium 1640 [+]L-glutamine) containing 10% (v/v) fetal bovine serum (FBS, from Atlanta Biologicals™, Flowery

Branch, GA) and 0.05 mM 2-mercaptoethanol (BME), supplemented with penicillin (100 U/mL), streptomycin (100 mg/mL), gentamicin sulfate (7 µg/mL), and 0.01 M bicarbonate. Primary human tracheal epithelial (NhTE) cells were provided by CF@LANTA Experimental Models Support Core and maintained at 37°C under 5% CO₂, humidified atmosphere. The NhTE cells were procured from de-identified lung donor organ transplant tissue that were deemed suitable for transplant into a recipient. The NhTE were plated in transwell plates, differentiated into ciliated, mucous producing cells, and sustained with epithelial-air liquid interface (E-ALI) media that was provided by the core. The protocol for isolating primary human tracheal epithelial cells was approved by the Emory University Institutional Review Board.

- 1.5. *Particle uptake by macrophages*: MH-S cells were subcultured from the working stock according to standard methods, removing the media and adding a 0.5% Trypsin-EDTA solution to promote cell detachment. The cell suspension was removed and centrifuged at 1800 RPM for 3 minutes, the supernatant aspirated, and the cell-pellet resuspended in ~3 mL fresh media. Cell counts were achieved via 0.4% Trypan blue (Invitrogen) exclusion assay performed in a Countess™ II FL Automated Cell Counter (Life Technologies™, now Invitrogen). Cells were then seeded into A8 glass chamber slides (Tab-Tek® II Chamber Slide™) at 80,000 cells/mL. Cells were allowed to seed for 24 h before treatment with 1, 5, 10, 15, and 20 nM DzNP, after which, were washed twice with sterile PBS, fixed in methanol, incubated with Silver Enhancement Stain (Ted Pella) for 5 minutes, mounted with Permount® (Fisher Scientific), and imaged using a Leica DM2700 Light Microscope.

- 1.6. *In vitro gene expression*: Subcultured MH-S cells were plated into 6-well and 12-well plates at 200,000 cells and 150,000 cells per mL, respectively. Cells were treated for 24 hours with 1.25, 2.5, 5, or 10 nM of 2251DzNP or 25, 50, 100, or 200 $\mu\text{g/ml}$ DSS. The cells were homogenized using the *mirVana* RNA isolation kit or TRIzol, both according to the manufacturers' protocols. The total purified RNA was used to generate cDNA using iScript cDNA synthesis kit, which was then combined with TaqMan® Gene Expression (Applied Biosystems) master mix and TaqMan® Assay probes for the target scavenger receptor gene of interest. Quantitative real-time PCR (qRT-PCR) was conducted in Applied Biosystems 7500 Fast Real-Time PCR System. Data were given as relative mRNA levels obtained by extrapolation of comparative C_t values from the slopes of the standard curve for each primer set using Applied Biosystems Sequence Detection System Software. Gene expression levels were then normalized to the endogenous housekeeping gene: 18S in MH-S cells and GAPDH in primary human cells. The qRT-PCR data were tabulated from 3 individual wells in a given experiment, repeated in biological triplicate, and analyzed globally for trends.
- 1.7. *Statistics*: GraphPad Prism 8 software was used to execute statistical analyses. Results were quantified and reported as mean \pm SEM. Data were statistically analyzed and compared using one-way analysis of variance (ANOVA) such that P values of less than 0.05 were considered significant.

III. Results

1.1. MARCO and MSR1 Gene Expression with Dose Response to DSS and DzNP in MH-S Cells:

To examine whether DSS exposure would stimulate or inhibit gene expression of SR-As, MH-S cells were subcultured and seeded in 6-well plates for 24 hours before treatment with 50 μ g/mL, 100 μ g/mL, and 200 μ g/mL high MW DSS (>500 kDa) in RPMI media. After 24 hours in treatment media, cells were harvested and analyzed for MARCO and MSR1 expression, two commonly found SR-As in macrophages. MARCO expression levels increased with exposure to high MW DSS exposure, with

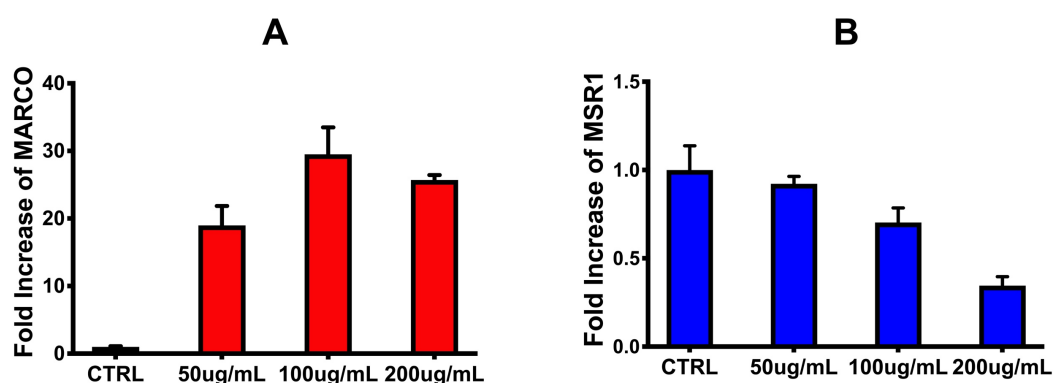


Figure 1: MH-S cells treated with dose-response of high MW DSS compared to media control. Values expressed as fold increase relative to control, reporting mean \pm SEM and N=3.

the maximum effect on expression at 100 μ g/mL (Figure 1A). When cells in high MW DSS were analyzed for MRS1 expression, MSR1 expression decreased in a dose-dependent manner (Figure 1B).

A similar setup as high MW DSS was used for low MW DSS (6.5-10 kDa) using 25 μ g/mL, 50 μ g/mL, 100 μ g/mL, 200 μ g/mL, and 5% (v/v) PBS to media vehicle, which was then analyzed for MARCO and MSR1 gene expression. MARCO gene expression exhibited a dramatic dose-dependent increase with low MW DSS (Figure 2A). Unlike high MW DSS, MSR1 expression levels increased with exposure to low

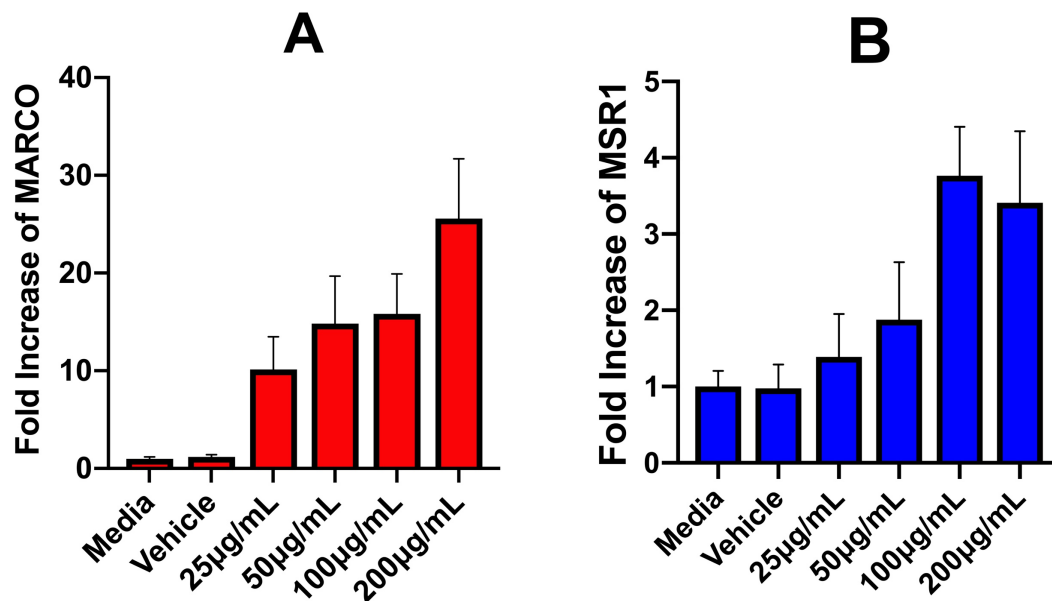


Figure 2: MH-S cells treated with dose-response of low MW DSS compared to media control. Values expressed as fold increase relative to control, reporting mean \pm SEM and N=3.

MW DSS. (Figure 2B). The difference in MSR1 response between low and high MW DSS suggests that the size of the DSS molecule has a direct impact on MSR1 gene regulation.

To determine whether exposure to DzNPs affected gene-expression of MARCO and MSR1, a dose-response treatment with 1.25nM, 2.5nM, 5nM, and 10nM 2251DzNP with 3% (v/v) PBS to media vehicle control was performed. MARCO gene expression dramatically increased with higher concentrations of DzNPs, similar to the findings with low and high MW DSS (Figure 3A). MSR1 gene expression followed

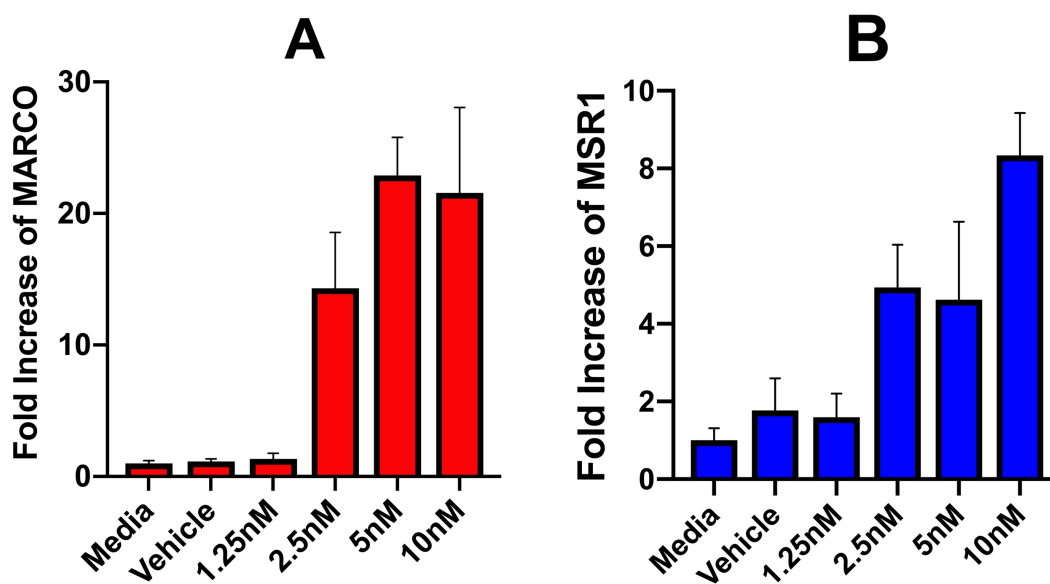


Figure 3: MH-S cells treated with 2251 DzNP dose-response, compared to media control. A) Expression levels of MARCO after treatment. B) Expression levels of MSR1 after treatment. Values expressed as fold increase relative to control, reporting mean \pm SEM and N=3.

a more linear increase with exposure to increasing DzNP concentrations (Figure 3B).

Taken together, this data suggests that both DSS and DzNP exposure directly affect gene expression in MARCO and MSR1, and the effect of DzNP on MARCO and MSR1 expression is similar to low MW DSS, but not high MW DSS, suggesting that DzNP regulation of SR-As is dependent on molecular charge ratio rather than size.

1.2. *MARCO and MSR1 Gene Expression for Concomitant 2251DzNP and low MW DSS in MH-S Cells:* To determine if SR inhibition with DSS would affect MARCO and MSR1 expression in MH-S cells concomitantly treated with DzNPs, cells were seeded in 12-

well plates for 24 hours and treated in media containing both 5nM 2251DzNP and 50 ug/mL low MW DSS and compared to 5nM 2251DzNP, 50 ug/mL high MW DSS, 4% (v/v) PBS vehicle, and media alone. MARCO and MSR1 expression levels were evaluated and both genes increased expression for treatment individually with 2251DzNP or low MW DSS, but when treated in the same well, had an overall decrease in expression (Figure 4). This data suggests that concomitant DSS administration can directly inhibit the stimulatory effects of DzNPs on MARCO and MSR1 gene expression in MH-S.

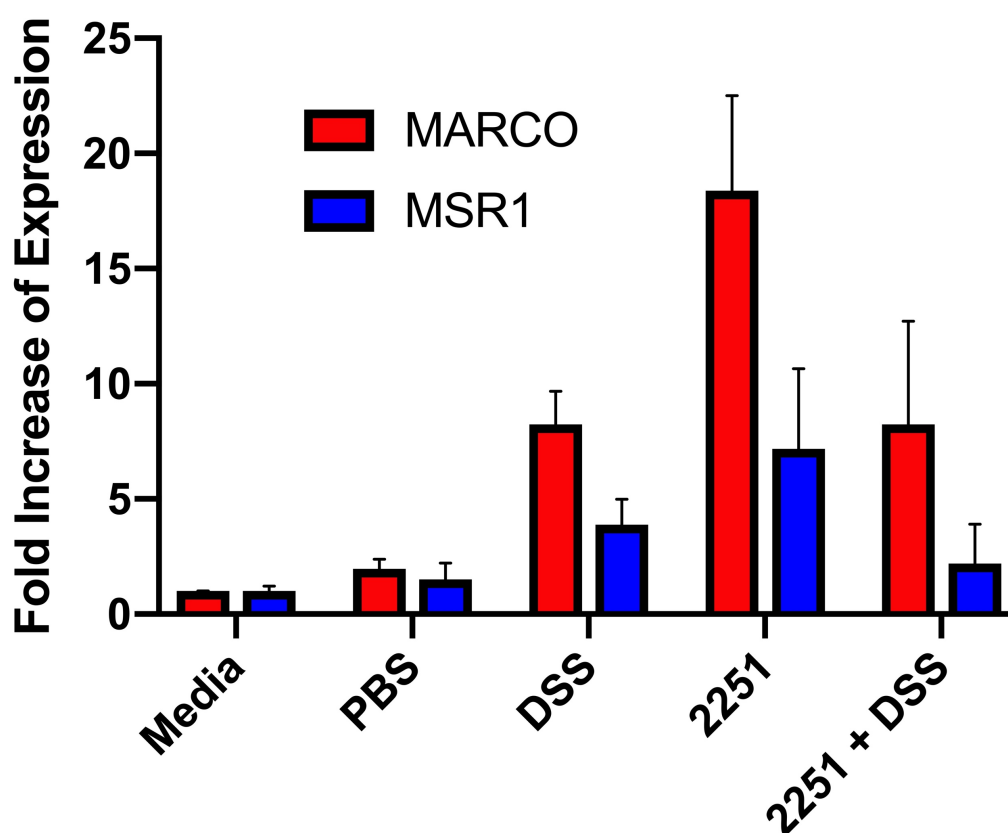


Figure 4: MH-S cells treated with 5nM 2251 DzNP, 50ug/mL low MW DSS, or both, compared to media control. Expression fold increase for the respective genes were set to independent control media values. Values expressed as fold increase relative to control, reporting mean \pm SEM and N=3.

1.3. *MARCO and MSR1 Expression Levels with Low Dose 2251DzNP in MH-S Cells*: Given the robust uptake of DzNPs in macrophages, even very low concentrations of DzNPs may have an effect on SR-A gene expression. To test this, cells were treated with 2251DzNP concentrations between 10pM and 2nM. Data for the MARCO gene expression continued to demonstrate an increase in gene expression with increasing

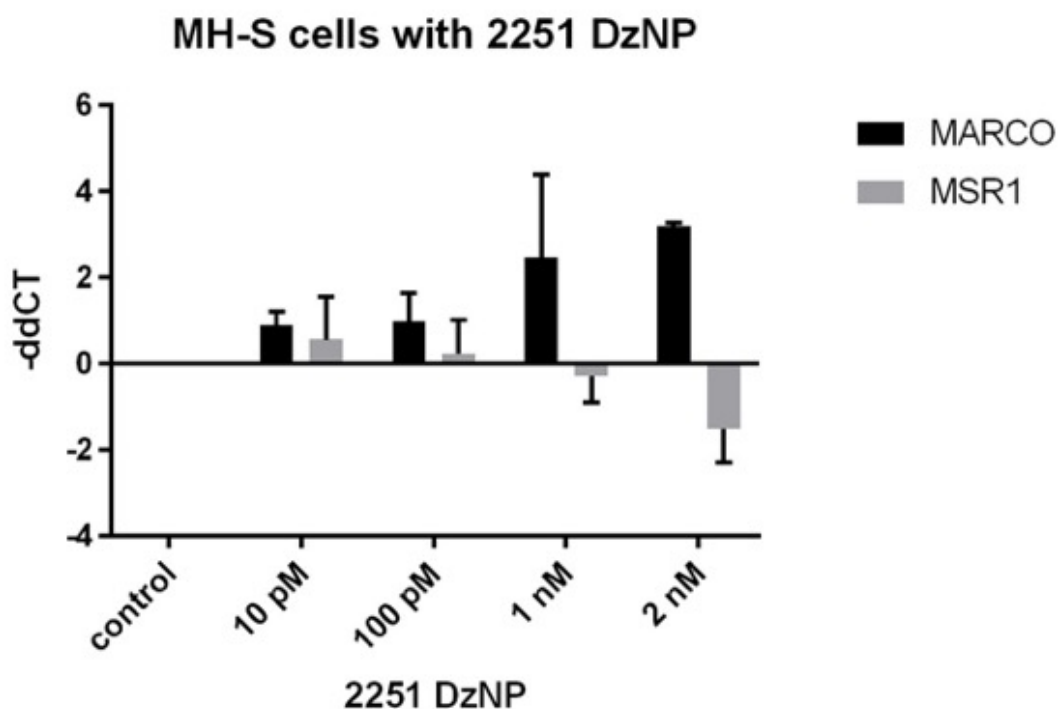


Figure 5: MH-S cells treated with low concentrations of 2251DzNP as compared to media control. Expression fold increase for the respective genes were set to independent control media values. Values expressed as -ddCt generated by qRT-PCR software. N=3.

doses of 2251DzNP. However, gene expression levels for MSR1 actually decreased relative to control media (Figure 5). The data suggests there is a biphasic response in MSR1 expression with DzNP exposure, with low concentrations decreasing MSR1 expression and high concentrations increasing MSR1 expression.

1.4. *MSR1 Expression in NhTE Cells with Concomitant Treatment*: Primary human tracheal epithelial (NhTE) cells were cultured in Transwell plates with polycarbonate membrane surfaces, which were provided by CF@LANTA Experimental Models Support Core. Upon sufficient cellular differentiation as marked by mucus secretion, plates were treated via two approaches: basal addition to the growth media or apical addition directly to the cell surface. Using 1xPBS at physiological pH as vehicle, 50 μ g/mL low MW DSS, 5nM 2251DzNP, or both simultaneously, cells for basal

MSR1 Expression in NhTE

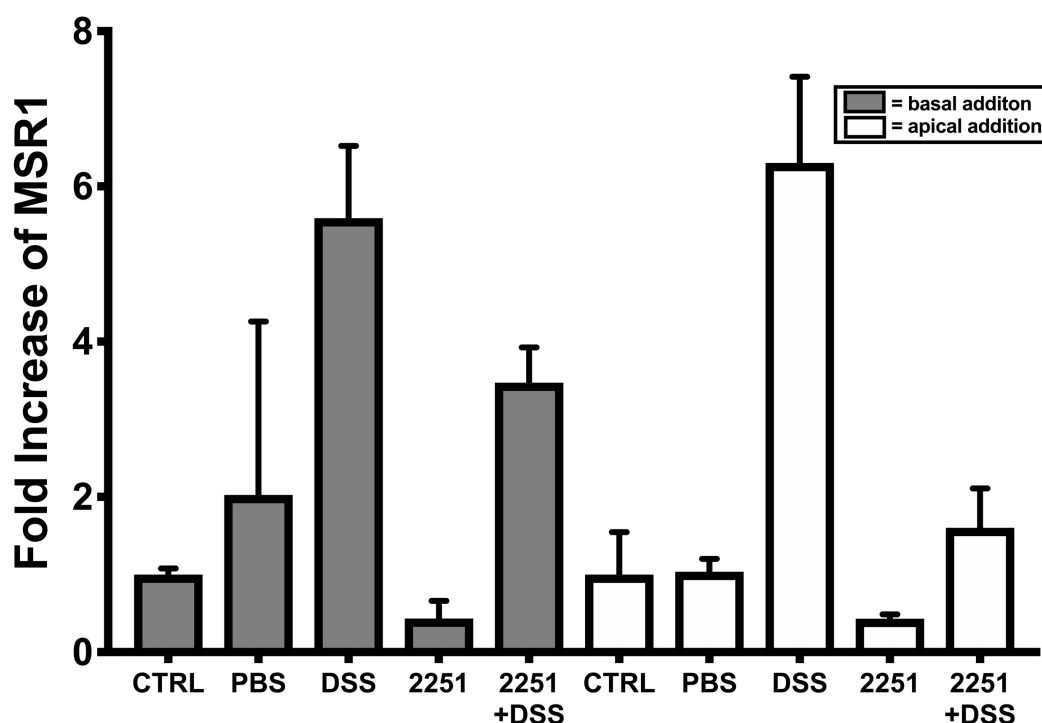


Figure 6: NhTE cells treated 5nM 2251 DzNP, 50 μ g/mL low MW DSS, or both, compared to media control. Respective additions were relative to independent control values. Values as fold increase relative to control, reporting mean \pm SEM and N=3.

addition received 600 μ L per treatment group with no media addition to the surface while apical addition received 40 μ L of treatment media directly to the cell surface and 600 μ L of normal media to the basal wells. In human airway epithelial cells,

addition of low MW DSS upregulates MSR1 whereas 2251DzNP downregulates MSR1 expression, each irrespective of basal or apical exposure, The concomitant addition of 2251DzNP and low MW DSS upregulates MSR1 expression but not to the same degree as DSS alone (Figure 6).

1.5. *CD36 and COLEC12 Expression in NhTE Cells with Concomitant Treatment:* NhTE cells provided by CF@LANTA were treated similarly to those that were analyzed for MSR1 gene expression. Applying the treatment media to the basal or apical side overall changed the magnitude of expression, reaching larger fold increase when applied to the apical surface. Basal addition of 2251DzNP increased COLEC12 fold change while low MW DSS decreased COLEC12 it; addition of both increased the expression levels of COLEC12, but not to the same extent as 2251DzNP alone(Figure 7A). Apical

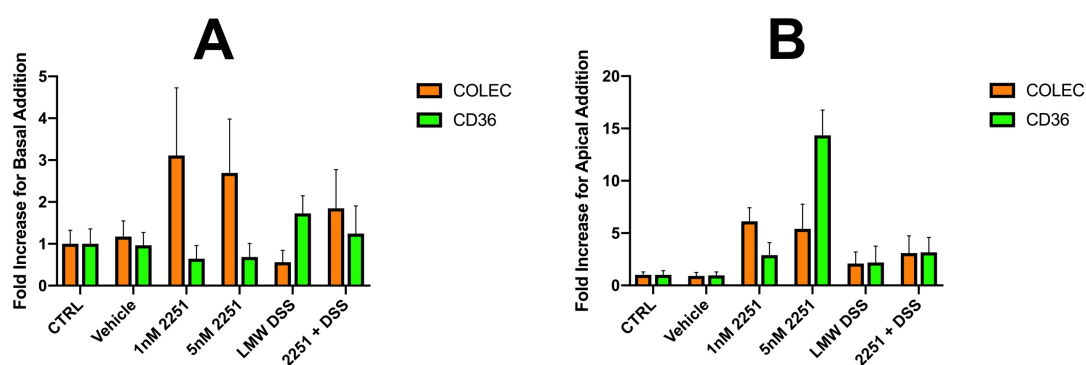


Figure 7: NhTE cells treated 5nM 2251 DzNP, 50ug/mL low MW DSS, or both, compared to media control. Respective gene expression levels were relative to independent control values. Values expressed as fold increase relative to control, reporting mean \pm SEM and N=2.

addition of either 2251DzNP or DSS increased COLEC12 expression. The combination of the two also increased COLEC12 expression, but not to the same extent as 2251DzNP alone (Figure 7B). CD36 expression decreased with 2251DzNP addition and increased for low MW DSS when each were added to the basal side, and when they were comitantly added (Figure 7A). When added apically, 2251DzNP

increased the expression of CD36 while low MW DSS and concomitant addition slightly increased expression (Figure 7B). Compared to the findings on the basal side, modulation of CD36 expression appears dependent upon basal or apical addition of 2251DzNP.

1.6. *MH-S Particle Uptake*: MH-S cells were seeded in A8 Chamber Slides and treated with increasing concentrations of 2251DzNP. Post-treatment, the cells were incubated in silver stain enhancement and fixed on the slides for image capture by light microscopy. Intensity of the silver staining increased with increasing concentrations of 2251DzNP indicating the cellular uptake of 2251DzNP is dose-dependent and that

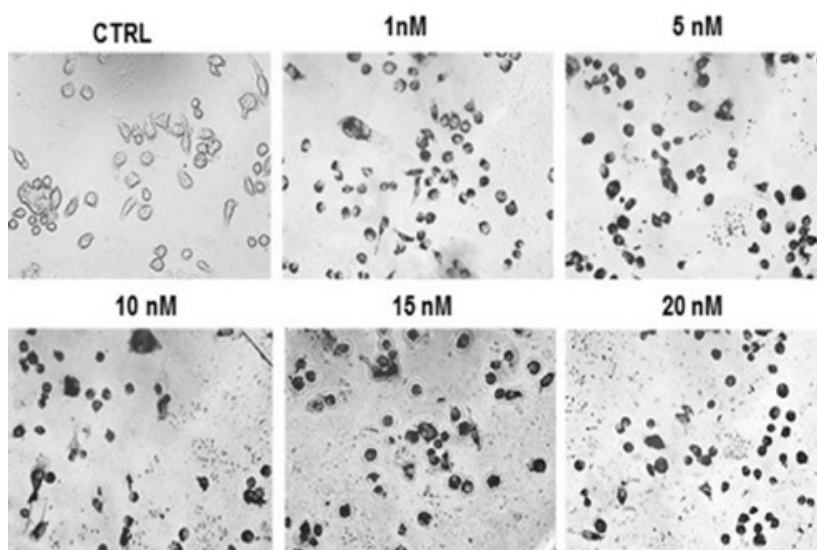


Figure 8: MH-S cells treated with dose-dependent 2251DzNP, fixed, stained, and DzNP uptake evaluated qualitatively.

nanomolar amounts of DzNP is sufficient to stimulate cellular uptake (Figure 8).

IV. Discussion

Pulmonary macrophages and airway epithelial cells are primarily responsible for the distribution of inhaled NPs in the lungs, including uptake, physiologic response, and subsequent removal[48]. The mechanism for NP uptake has been investigated in multiple cell types, displaying a range of uptake pathways that depend on the NPs' specific properties and how it interacts with the cell membrane[39, 47, 51]. The size and shape of NPs influence their ability to travel to a particular region in the body, such as the alveolar space, whereas the chemical nature and surface coatings of NPs significantly impact how cells interact with NPs. Scavenger receptor-mediated endocytosis is the predominantly described uptake pathway for most NPs[48]. However, the uptake mechanism of DNAzyme-conjugated nanoparticles remains poorly understood in the lungs.

To optimize drug delivery and further the therapeutic potential of DzNPs, identifying which SRs are involved in cellular uptake in the lung is necessary. We reported that both DzNPs and a known SR blocker dextran sodium sulfate (DSS) modulate SR-A expression in alveolar macrophages and SR-A/B expression in airway epithelial cells. SR-As are uniquely important for the uptake of oligonucleotide-AuNP conjugates in kidney and HeLa cells[51]. Our data supports the involvement of SR-As in DzNP uptake as gene expression levels increase when treated with both 2251DzNP and DSS. Interestingly, high MW DSS causes a decrease in MSR1 expression whereas low MW DSS causes an increase. High MW DSS is believed to shrink and wrap in on itself in a highly ionized solution. The low MW DSS has significantly less branching and regularly linearizes in solution, mimicking the helical structure and charge distribution of DNA and RNA. These properties are likely responsible for low MW DSS's ability to release DNA from histones, inhibit RNA binding to ribosomes,

and inhibit DNA binding to DNA polymerase III during PCR[61]. The data presented corroborate the hypothesis that DzNPs and low MW DSS are viewed similarly by the cell and that SR-As are necessary receptors for linear oligonucleotide recognition in alveolar macrophages.

The increased expression of both MARCO and MSR1 in MH-S cells in response to increasing concentrations of 2251DzNP or low MW DSS may be necessary to increase endocytosis of the ligand or to maintain receptor density on the cell membrane. Increased MARCO and MSR1 expression after DzNP or DSS exposure may also signify an inflammatory response; however, current literature suggests that DSS does not directly initiate inflammatory pathways. Although inflammation may be induced as a consequence of DSS disruption of cell monolayers allowing entry of bacteria and other inducers of inflammation, this is an unlikely mechanism of inflammation in MH-S cells because they do not form monolayers[62].

While 2251DzNP and low MW DSS individually increase MARCO and MSR1 expression, concomitant treatment with 2251DzNP and low MW DSS does not have an additive effect on MARCO and MSR1 expression. Increases in MARCO and MSR1 expression with concomitant treatment closely reflect the expressions levels seen with low MW DSS alone, suggesting DSS is preferentially recognized by MARCO/MSR1 or there is a higher DSS ligand to receptor molecular ratio with the concentrations of DSS and DzNP used.

SR expression in airway epithelial cells is poorly described in the literature but knowing what SR receptors are present is essential to understanding the mechanisms of DzNP uptake in airway epithelium. In the data presented, airway epithelial cells express

MSR1 but not MARCO similar to previously reported data in airway epithelial cells[63]. MSR1 expression in NhTE cells in response to low MW DSS increased similarly to MH-S cells; however, MSR1 expression was inhibited by DzNP in NhTE cells in contrast to MH-S cells regardless of whether DzNP was added to the apical or basal surface. These findings suggest that MSR1 may not play a large role in DzNP uptake in airway epithelium. Because NhTE cells form a tight monolayer in culture, the effects of DSS on MSR1 may be a consequence of monolayer disruption rather than a direct stimulatory effect.

Little is known about scavenger receptors other than class A scavenger receptors in the lung. Interestingly, we found CD36, a class B scavenger receptor, and COLEC12, a Class E scavenger receptor, were expressed in airway epithelial cells[44]. Class-B SRs recognize similar ligands to SR-A but represent specialized motifs that potentiate inflammatory responses within cells. Given that CD36 expression is only mildly changed with exposure to DzNP or DSS, CD36 may not be heavily involved in the internalization of DzNPs or similarly charged nanozymes[64]. The increase in CD36 expression with low MW DSS exposure also suggests that the effect of low dose DSS is not specific to one class of scavenger receptors or that CD36 expression is a consequence of monolayer disruption. The increased expression in COLEC12 with 251DzNP is a novel finding, but the role of COLEC 12 in DzNP uptake still needs to be defined. The upregulation in COLEC12 may simply illustrate the complex relationship the SR classes have with one another.

The data present are limited to only gene expression; localization of SRs on the cell membrane is still needed to support the hypothesis that DzNPs are internalized by binding with specific SRs. At the moment, modulated expression levels are assumed to correspond to modulated protein expression. Going forward, confirming cell surface localization of SRs

can be accomplished using immunocytologic techniques. Uptake inhibition assays using DSS and quantitative analysis of immunologic biomarkers will give more insight into the precise mechanism of action for endocytosis of DzNPs. Comparison of DSS to other known SR inhibitors using known ligands, such as polyinosinic acid or other suitable oligonucleotides, can help differentiate between a direct binding and internalization of DzNPs versus indirect stimulation of SR expression by inflammation.

DzNPs have vast potential as novel therapeutics and as vehicles for enhanced drug delivery. As such, it is critical to understand how nanoparticles and DzNPs are taken up into cells. The data presented demonstrate that DzNPs regulate expression of scavenger receptors in the lung, that alveolar macrophages have high affinity for DzNPs, and that MSR1 and/or COLEC12 may be important SRs for DzNP uptake in airway epithelium. The data also illustrate that complex interactions between classes of SRs need to be considered when defining the uptake mechanisms of DzNPs.

V. References

1. Buzea, C., I.I. Pacheco, and K. Robbie, *Nanomaterials and nanoparticles: Sources and toxicity*. *Biointerphases*, 2007. **2**(4): p. MR17-MR70.
2. Alemán, J., et al., *Definitions of Terms Relating to the Structure and Processing of Sols, Gels, Networks, and Inorganic-Organic Hybrid Materials*. *Pure and Applied Chemistry*, 2007. **79**(10): p. 1801-1829.
3. Qian, C., et al., *Identification of Nanoparticles via Plasmonic Scattering Interferometry*. *Angewandte Chemie*, 2019. **58**(13): p. 4217-4220.
4. Thanh, N.T. and L.A. Greenab, *Functionalisation of nanoparticles for biomedical applications*. *Nanotoday*, 2010. **5**(3): p. 213-230.
5. Binnig, G. and H. Rohrer, *Scanning Tunneling Microscopy*. *Surface Science*, 1983. **126**: p. 236-244.
6. Chen, C.J., *Introduction to Scanning Tunneling Microscopy*. 2 ed. 2006, New York City, NY: Oxford University Press.
7. Klasen, H.J., *Historical review of the use of silver in the treatment of burns. I. Early uses*. *Burns*, 2000. **26**(2): p. 117-130.
8. Luan, Z., et al., *Mesopore Molecular Sieve MCM-41 Containing Framework Aluminum*. *Journal of Physical Chemistry*, 1995. **99**(3): p. 1018-1024.
9. Alivisatos, A.P., *Semiconductor Clusters, Nanocrystals, and Quantum Dots*. *Science*, 1996. **271**(5251): p. 933-937.
10. Stevenson, R., et al., *Nanoparticles and inflammation*. *Scientific World Journal*, 2011. **11**: p. 1300-12.
11. Chen, G., et al., *Nanochemistry and Nanomedicine for Nanoparticle-based Diagnostics and Therapy*. *Chemical Reviews*, 2016. **116**(5): p. 2826-85.
12. Hassellöv, M., et al., *Nanoparticle analysis and characterization methodologies in environmental risk assessment of engineered nanoparticles*. *Ecotoxicology*, 2008. **17**: p. 344-361.
13. Zahid, M., et al., *DNA nanotechnology: a future perspective*. *Nanoscale Research Letters*, 2012. **8**(1): p. 119-132.
14. Seeman, N.C., *Nanomaterials Based on DNA*. *Annual Review of Biochemistry*, 2010. **79**: p. 65-87.

15. Breaker, R.R. and G.F. Joyce, *The expanding view of RNA and DNA function*. Chemistry & Biology, 2014. **21**(9): p. 1059-1065.
16. Kruger, K., et al., *Self-Splicing RNA—Autoexcision and Autocyclization of the Ribosomal RNA Intervening Sequence of Tetrahymena*. Cell, 1982. **31**: p. 147-157.
17. Agrawal, N., et al., *RNA Interference: Biology, Mechanism, and Applications*. Microbiology and Molecular Biology Reviews, 2003. **67**(4): p. 657-685.
18. Sun, L.Q., et al., *Catalytic Nucleic Acids-From Lab to Applications*. Pharmacological Reviews, 2000. **52**(3): p. 325-347.
19. Breaker, R.R., *DNA enzymes*. Nature Biotechnology, 1997. **15**: p. 427-431.
20. Silverman, S.K., *Catalytic DNA (deoxyribozymes) for synthetic applications-current abilities and future prospects*. Chemical Communications, 2008(30): p. 3467-85.
21. Joyce, G.F., *Directed evolution of nucleic acid enzymes*. Annual Review of Biochemistry, 2004. **73**: p. 791-836.
22. Dass, C.R., et al., *Cellular Uptake, Distribution, and Stability of 10-23*. Antisense and Nucleic Acid Drug Development, 2002. **12**: p. 239-299.
23. Fokina, A.A., D.A. Stetsenko, and J.-C. François, *DNA enzymes as potential therapeutics: towards clinical application of 10-23 DNazymes*. Expert Opinion on Biological Therapy, 2015. **15**(5): p. 689-711.
24. Ven, K., et al., *Re-engineering 10-23 core DNA- and MNazymes for applications at standard room temperature*. Analytical and Bioanalytical Chemistry, 2019. **411**(1): p. 205-215.
25. Yehl, K., et al., *Catalytic Deoxyribozyme-Modified Nanoparticles for RNAi-Independent Gene Regulation*. ACS Nano, 2012. **6**(10): p. 9150-9157.
26. Petree, J.R., et al., *Site-Selective RNA Splicing Nanozyme: DNzyme and RtcB Conjugates on a Gold Nanoparticle*. ACS Chemical Biology, 2018. **13**: p. 215-224.
27. Silverman, S.K., *Deoxyribozymes: DNA catalysts for bioorganic chemistry*. Organic & Biomolecular Chemistry 2004. **2**(19): p. 2701-6.
28. Fokina, A.A., et al., *Targeting Insulin-like Growth Factor I with 10-23 DNazymes: 2'-O-Methyl Modifications in the Catalytic Core Enhance mRNA Cleavage*. ACS Biochemistry, 2012. **51**: p. 2181-2191.

29. Sel, S., et al., *Effective prevention and therapy of experimental allergic asthma using a GATA-3-specific DNAzyme*. *Journal of Allergy and Clinical Immunology*, 2008. **121**(4): p. 910-916 e5.
30. Somasuntharam, I., et al., *Knockdown of TNF-alpha by DNAzyme gold nanoparticles as an anti-inflammatory therapy for myocardial infarction*. *Biomaterials*, 2016. **83**: p. 12-22.
31. Cho, K., et al., *Therapeutic nanoparticles for drug delivery in cancer*. *Clinical Cancer Research*, 2008. **14**(5): p. 1310-6.
32. Poupot, R., D. Bergozza, and S. Fruchon, *Nanoparticle-Based Strategies to Treat Neuro-Inflammation*. *Materials*, 2018. **11**(2).
33. Zagorovsky, K. and W.C. Chan, *A Plasmonic DNAzyme Strategy for Point-of-Care Genetic Detection of Infectious Pathogens*. *Angewandte Chemie*, 2013. **125**(11): p. 3250-3253.
34. Zhou, W., J. Ding, and J. Liu, *Theranostic DNAzymes*. *Theranostics*, 2017. **7**(4): p. 1010-1025.
35. Wang, X., Y. Hua, and H. Wei, *Nanozymes in bionanotechnology: from sensing to therapeutics and beyond*. *Inorganic Chemistry Frontiers*, 2016. **3**: p. 41-60.
36. Xiang, Y., et al., *DNAzyme-functionalized gold nanoparticles for biosensing*. *Advances in Biochemical Engineering/Biotechnology*, 2014. **140**: p. 93-120.
37. Yin, B.C., et al., *DNAzyme self-assembled gold nanoparticles for determination of metal ions using fluorescence anisotropy assay*. *Analytical Biochemistry*, 2010. **401**(1): p. 47-52.
38. Sun, Y. and Y. Xia, *Shape-Controlled Synthesis of Gold and Silver Nanoparticles*. *Science*, 2002. **298**(5601): p. 2176-2179.
39. Ryoo, S.R., et al., *Functional delivery of DNAzyme with iron oxide nanoparticles for hepatitis C virus gene knockdown*. *Biomaterials*, 2012. **33**(9): p. 2754-61.
40. Ryoo, S.R., et al., *Multifunctional Nanoparticles for DNAzyme Delivery: Towards New Hepatitis C Drug*. *Molecular Therapy*, 2009. **17**: p. S259-S260.
41. Athar, M. and A.J. Das, *Therapeutic nanoparticles: State-of-the-art of nanomedicine*. *Reviews on Advanced Materials Science*, 2014. **1**(1): p. 25-37.

42. KG, S.B.G.C., *Efficacy, Safety, Tolerability, Pharmacokinetics and Pharmacodynamics Study of the Topical Formulation SB011 Applied to Lesional Skin in Patients With Atopic Eczema*, in *Clinical Trials*. 2017: United States.
43. Prabhudas, M., et al., *Standardizing scavenger receptor nomenclature*. *Journal of Immunology*, 2014. **192**(5): p. 1997-2006.
44. PrabhuDas, M.R., et al., *A Consensus Definitive Classification of Scavenger Receptors and Their Roles in Health and Disease*. *Journal of Immunology*, 2017. **198**(10): p. 3775-3789.
45. Zani, I.A., et al., *Scavenger receptor structure and function in health and disease*. *Cells*, 2015. **4**(2): p. 178-201.
46. Steinbrecher, U.P., et al., *Recognition of Oxidized Low Density Lipoprotein by the Scavenger Receptor of Macrophages Results from Derivatization of Apolipoprotein B by Products of Fatty Acid Peroxidation*. *The Journal of Biological Chemistry*, 1989. **24**(26): p. 15216-15223.
47. Mukhopadhyay, S., et al., *SR-A/MARCO-mediated ligand delivery enhances intracellular TLR and NLR function, but ligand scavenging from cell surface limits TLR4 response to pathogens*. *Blood*, 2011. **117**(4): p. 1319-1328.
48. Shannahan, J.H., W. Bai, and J.M. Brown, *Implications of scavenger receptors in the safe development of nanotherapeutics*. *Receptors & Clinical Investigation*, 2015. **2**(3): p. e811.
49. Yew, K.H., B. Carsten, and C. Harrison, *Scavenger receptor A1 is required for sensing HCMV by endosomal TLR-3/-9 in monocytic THP-1 cells*. *Molecular Immunology*, 2010. **47**(4): p. 883-93.
50. Love, R.J., et al., *An investigation of scavenger receptor A mediated leukocyte binding to polyanionic and uncharged polymer hydrogels*. *Journal of Biomedical Materials Research Part A*, 2015. **103**(5): p. 1605-12.
51. Patel, P.C., et al., *Scavenger receptors mediate cellular uptake of polyvalent oligonucleotide-functionalized gold nanoparticles*. *ACS Bioconjugate Chemistry*, 2010. **21**(12): p. 2250-6.

52. Baid, K., et al., *Direct binding and internalization of diverse extracellular nucleic acid species through the collagenous domain of class A scavenger receptors*. Immunology & Cell Biology, 2018. **96**(9): p. 922-934.
53. Bakand, S., A. Hayes, and F. Dechsakulthorn, *Nanoparticles: a review of particle toxicology following inhalation exposure*. Inhalation Toxicology, 2012. **24**(2): p. 125-135.
54. Holgate, S.T., et al., *Asthma*. Nature Reviews Disease Primers, 2015. **1**: p. 15025.
55. Banks, W. and C.T. Greenwood, *Physical Properties of Solutions of Polysaccharides*. Advances in Carbohydrate Chemistry, 1963. **18**: p. 357-398.
56. Katchalsky, A., *Polyelectrolytes and Their Biological Interactions*. Biophysical Journal, 1964. **4**(2): p. 9-41.
57. Sanders, F.K. and J.D. Smith, *Effect of collagen and acid polysaccharides on the growth of BHK-21 cells in semi-solid media*. Nature, 1970. **227**(5257).
58. Wahl, G.M., M. Stern, and G.R. Stark, *Efficient transfer of large DNA fragments from agarose gels to diazobenzyloxymethyl-paper and rapid hybridization by using dextran sulfate*. PNAS, 1979. **76**(8): p. 3683-3687.
59. Lindberg, B. and S. Svensson, *Structural Studies on Detran from Leuconostoc mesenteroids NRRL-B-512*. ACTA Chemica Scandinavica, 1968. **22**: p. 1907-19012.
60. Hill, H.D. and C.A. Mirkin, *The bio-barcode assay for the detection of protein and nucleic acid targets using DTT-induced ligand exchange*. Nature Protocols, 2006. **1**(1): p. 324-336.
61. Kerr, T.A., et al., *Dextran sodium sulfate inhibition of real-time polymerase chain reaction amplification: a poly-A purification solution*. Inflammatory Bowel Diseases, 2012. **18**(2): p. 344-8.
62. Laroui, H., et al., *Dextran sodium sulfate (DSS) induces colitis in mice by forming nano-lipocomplexes with medium-chain-length fatty acids in the colon*. PLoS One, 2012. **7**(3): p. e32084.
63. Sapkota, M., et al., *Malondialdehyde-acetaldehyde (MAA) adducted surfactant protein induced lung inflammation is mediated through scavenger receptor a (SR-A1)*. Respiratory Research, 2017. **18**: p. 36-46.

64. Batista, C.A.S., R.G. Larson, and N.A. Kotov, *Nonadditivity of nanoparticle interactions*. Science, 2015. **350**(6257): p. 176-186.